Quantum critical benchmark for electronic structure theory

Paul E. Grabowski and Kieron Burke

Phys. Rev. A **91**, 032501 — Published 3 March 2015

DOI: 10.1103/PhysRevA.91.032501

Quantum critical benchmark for electronic structure theory

Paul E. Grabowski[1,*] and Kieron Burke[2,†]

[1] *Department of Chemistry, University of California, Irvine, CA 92697, USA*
[2] *Departments of Chemistry and Physics, University of California, Irvine, CA 92697, USA*

Two electrons at the threshold of ionization represent a severe test case for electronic structure theory. Variational methods can yield highly accurate energies, but may be less accurate for other operators of interest. A pseudospectral method yields very accurate expectations values for the two-electron ion with nuclear charge at and close to the critical value which yields zero ionization energy. As an illustration, the ground-state density is calculated and an extremely accurate parametrization given. Other components in Kohn-Sham density functional theory are also calculated, and the efficacy of approximations discussed.

I. INTRODUCTION

The value of highly accurate benchmark calculations to first-principles electronic structure theory cannot be overstated. While comparison with experiment is the ultimate arbiter of the usefulness of prediction, the ability to control and eliminate multiple sources of error with a direct solution of the Schrödinger equation allows pure 'apples-to-apples' comparisons. The two-electron atom is one of the simplest nontrivial quantum systems and so serves as a common test problem for electronic structure methods, from early variational [1] and computer [2] calculations to more recent basis set comparisons [3] and ultra-high precision calculations [4–6]. The special case when the ionization potential is precisely zero, i.e., the nuclear charge Z_c is the smallest value that binds two electrons, is the simplest case of a quantum-critical electronic problem [7]. Such systems have been mapped to phase transitions in statistical mechanics [8]. In this limit, the electron positions are most strongly correlated with each other and the decay of the electron density is slowest, two issues that are difficult for electronic structure methods to handle. Recently, high-precision variational calculations have greatly expanded the accuracy to which Z_c is known [9], and strong correlation methods have been tested on this system [10].

For many N-electron atoms, there exists a minimum $Z_c = N - 1 - \nu$, with $0 < \nu < 1$, such that the ground state of $\hat{H}(Z)$ has positive ionization energy for all nuclear charges $Z > Z_c$. It is thought that $\lambda_c = 1/Z_c$ corresponds to the radius of convergence of the perturbative solution of the two-electron atom with the perturbation being the electron-electron interaction $1/r_{12}$ [11]. Baker and coworkers used 401 orders of perturbation theory to obtain $Z_c = 0.911\,03$ [11] and Ivanov later used better extrapolation techniques on their data to get $Z_c = 0.911\,028\,26$ [12]. From a direct variational calculation to solve for the critical charge, Sergeev and Kais obtained $Z_c = 0.911\,028\,225$ [13]. Recently, Estienne and coworkers [9] obtained $Z_c = 0.911\,028\,224\,077\,255\,73(4)$, far surpassing the prior estimates in precision. We obtain $Z_c = 0.911\,028\,224\,07(6)$, agreeing with Ref. [9] and an unpublished figure by Schwartz [14]. Although our Z_c is not as precise, our wave function is roughly as accurate as our value of Z_c (to about 10^{-10} of the maximum, even in the tail). Variational expansions typically have half as many accurate digits of accuracy in the wave function as in the energy [15]. Beyond ground-state energy comparisons, the density and expectation values can provide detailed information for strengths and weaknesses of electronic structure methods. The pioneering work of Umrigar and coworkers [16, 17] for several spherical atoms is a case in point. The availability of the Kohn-Sham (KS) potential and its eigenvalues was useful for all of density functional theory (DFT), and especially for the development of linear-response time-dependent density functional methods for finding excited state energies, where the ground-state orbitals and energies are vital inputs [18, 19].

In this article, we give a high-order expansion for the electron density at large r for all $Z \geq Z_c$, including fits for the ionization energy and the normalization factor. This information encodes the quantum critical transition. We give a highly accurate fit to the density for $Z = Z_c$ for all r as well as precise expectation values. We conclude with an example from DFT. Common semi-local energy functionals fail to capture the qualitative behavior of the correlation energy as $Z \to Z_c$, but this error is almost perfectly cancelled by their exchange approximations. We explain this cancellation in terms of the locality of the exchange-correlation holes.

II. METHOD

Standard quantum methods typically have trouble calculating states near the ionization threshold because of their much more diffuse and, hence, spatially correlated wave function, Ψ, and the accidental mixing of energetically similar continuum states into the ground state. For example, diffusion Monte Carlo calculations take advantage of the separation in energy between the ground and excited states and fails to separate degenerate states. However, the pseudospectral method used here is a non-

* paul.grabowski@uci.edu
† kieron@uci.edu

variational collocation method in which the value of Ψ is calculated on a grid in such a way that the *local* error in Ψ becomes exponentially small with increasing grid resolution. We accurately calculate the bound state right on the threshold of the continuum by automatically selecting normalizable states. Thus our method is particularly well-suited to produce benchmark expectation values for quantities not directly related to the energy at the critical value.

Pseudospectral methods [20] have their origins in fluid dynamics [21], where they are used to evolve systems without shocks because their convergence properties hold only for $\mathcal{C}^\infty$ functions. They have been extended to solving Einstein's field equations for colliding black holes by the excision of the singularities from the computational domain [22, 23]. In quantum chemistry, Friesner and others have shown orders of magnitude improvement in speed for a wide variety of methods [24–32]. Direct solution of Schrödinger's equation has been performed for one-electron problems [33, 34], but only recently has a sufficient representation of the computational domain been demonstrated for fully-correlated, two-electron atoms [35, 36]. We use the implementation of Ref. [36].

III. ASYMPTOTIC BEHAVIOR AND DENSITY FIT

A difficult test for any method is the large-r behavior of the density. As $r \to \infty$, for $Z > Z_c$, the well-known analysis of the exponential decay of the density [37] yields $n(r) \to \exp(-2\sqrt{2I}r)$, where I is the ionization energy. However, for $Z = Z_c$, the behavior differs qualitatively [$n(r) \to \exp(-4\sqrt{2(1-Z_c)}r)$, note, r is inside the square root]. For low values of Z, the asymptotic value is not approached until very large r. So one must use higher order expansions to connect the limits with our numeric results.

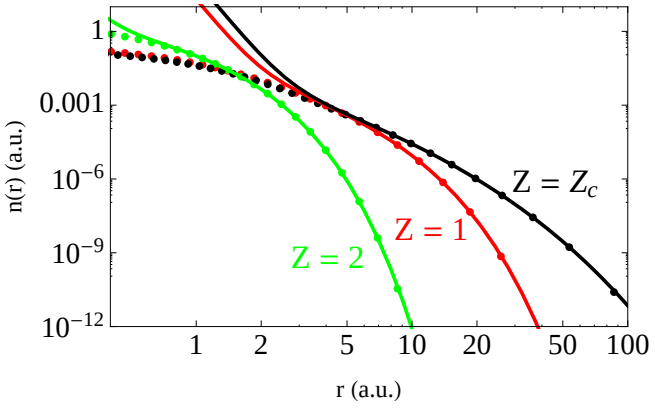

FIG. 1. (Color online) Exact (dots) and asymptotic ($A_1 = 5.528 \times 10^{-3}$, $A_2 = 1.517$, and $B = 0.1375$) densities (solid line) for $Z = 1, 2$, and Z_c.

To analyze these results, we review well-known facts from KS DFT[38]. The KS equations describe fictitious non-interacting fermions sitting in a potential, $v_{\rm S}(\mathbf{r})$, whose density matches the real one. For two spin-unpolarized electrons, one orbital is doubly occupied and the KS equation in atomic units is

$$\left[-\frac{1}{2}\nabla^2 + v_s(\mathbf{r})\right]\phi(\mathbf{r}) = \epsilon\phi(\mathbf{r}), \tag{1}$$

where $\phi = \sqrt{n(r)/2}$ and $\epsilon = -I = E + Z^2/2$ are the KS orbital and its energy, respectively, while $v_s(r)$ is the Kohn-Sham potential given by

$$v_s(\mathbf{r}) = -\frac{Z}{r} + v_{\rm H}(\mathbf{r}) + v_{\rm X}(\mathbf{r}) + v_{\rm C}(\mathbf{r}). \tag{2}$$

For two electrons, the Hartree and exchange potentials are trivially related,

$$v_{\rm H}(\mathbf{r}) = -2\,v_{\rm X}(\mathbf{r}) = \int \frac{n(\mathbf{r}')d\mathbf{r}'}{|\mathbf{r}-\mathbf{r}'|}, \tag{3}$$

and the correlation potential is defined so as to make Eq. (1) exact. For large r, the exchange potential, behaves as $-1/r$ while the correlation potential decays much faster, as $-\alpha/2r^4$, where α is the dipole polarizability of the $N-1$ system, here equal to $9/2Z^4$ [16]. Amovilli and March [39] derived the asymptotic behavior of the density at large r for $Z = 2$. We extend their work to any $Z > Z_c$ and to the next highest order in $1/r$ by solving Eq. (1) order by order:

$$\sqrt{n_Z(r)} \sim \frac{x^\beta\sqrt{A_Z}}{e^x}\left[\sum_{k=0}^{4}\frac{a_k}{x^k} - \frac{3r^{-2}}{4Z^4}\sum_{k=1}^{2}\frac{\tilde{a}_k}{x^k} + \mathcal{O}\left(x^{-5}\right)\right], \tag{4}$$

where $x = \eta\, r$, $\eta = \sqrt{2I}$, $\beta = \xi/\eta - 1$, and $\xi = Z - 1$. The normalization factor A_Z is defined as $A_Z = \lim_{r\to\infty} n_Z(r)\, e^{2x}/x^{2\beta}$. The formula

$$A_Z = \alpha_1\delta + \alpha_2\delta^2 + \alpha_3\delta^3, \tag{5}$$

with $\delta = Z - Z_c$, $\alpha_1 = 0.006\,674\,48$, $\alpha_2 = 0.567\,102$, and $\alpha_3 = 2/\pi$, fits our densities over the entire Z range to within 0.2% with the maximum error occurring around $Z = 1$. The value of α_3 comes from the large-Z limit of the density. Likewise,

$$I = \{1 + \beta_1\exp[-\beta_2\ln^2(\beta_3\delta)]\}(\beta_4\delta + \delta^2/2), \tag{6}$$

with $\beta_1 = 0.085\,704\,8$, $\beta_2 = 0.166\,941$, $\beta_3 = 5.097\,253$, and $\beta_4 = 2\langle 1/r_1\rangle_{Z=Z_c} - Z_c = 0.245\,189\,01$ has a maximum error of 0.3% occurring around $Z = 0.92$. The coefficients in the large-r expansion are given recursively as $a_0 = 1$, $a_k = -a_{k-1}[\xi - k\eta][\xi - (k-1)\eta]/(2k\eta^2)$, and $\tilde{a}_1 = 1$ and $\tilde{a}_2 = -(\beta^2 + \beta + 3)/2$.

At Z_c, the long range behavior changes [10, 39, 40]. Here we extend such asymptotic forms to higher order:

$$\sqrt{n_{Z_c}(r)} \sim \frac{\sqrt{B}e^{-y}}{r^{3/4}}\left[\sum_{k=0}^{8}\frac{b_k}{y^k} - \frac{9r^{-2}}{4Z_c^4}\sum_{k=1}^{4}\frac{\tilde{b}_k}{y^k} + \mathcal{O}\left(y^{-9}\right)\right], \tag{7}$$

n_0	0.23819008067	B	0.1375
c_1	0.0610986	c_2	0.0352145
c_3	−0.0494222	c_4	0.123575
c_5	−0.212456	c_6	0.308266
c_7	−0.328053	c_8	0.219550
d_1	7.82582×10^{-5}	d_2	3.79484
s	4.19599		

TABLE I. Parameters for Eq. (8) in atomic units.

where $B = \lim_{r\to\infty} n_{Z_c}(r) e^{2y} r^{3/2} \approx 0.1375$, $y = 2\sqrt{2|\xi_c|r}$, $\xi_c = Z_c - 1$, and $b_0 = 1$, $b_k = -b_{k-1}(2k+1)(2k-3)/8k$, while $\tilde{b}_1 = 4/5$, $\tilde{b}_2 = -17/10$, $\tilde{b}_3 = 1107/224$, and $\tilde{b}_4 = -30\,489/1792$. These asymptotic expressions are shown with our calculated densities in Fig. 1 for $Z = Z_c, 1$ and 2. See appendix A for the errors in this expansion.

To make our results more immediately useful , we created a fit to the critical density:

$$n_{Z_c}(r) = \left[n_0 e^{-2Z_c r} \left(1 + \sum_{k=1}^{8} \frac{c_k}{2^{k^2/4}} r^{k+1} \right) + B \frac{r^3}{s^3 + r^3} \left(\frac{a}{\tilde{y}} \right)^3 \frac{e^{-\tilde{y}}}{1 - \frac{3}{2\tilde{y}} + \frac{21}{8\tilde{y}^2} - \frac{87}{16\tilde{y}^3} + \frac{1755}{128\tilde{y}^4}} \right] \left[1 + \frac{d_1 r^{10}}{1 + d_2 r^{29/2}} \right], \quad (8)$$

	$Z = Z_c$	$Z = 2$ Ref. [36]
$\langle r_1^2 \rangle$	39.779 95(20)	1.193 482 995 30(16)
$\langle r_{12}^2 \rangle$	81.303 37(40)	2.516 439 313 8(6)
$\langle \boldsymbol{r}_1 \cdot \boldsymbol{r}_2 \rangle$	-0.871 728 2(66)	-0.064 736 661 60(25)
$\langle r_1 \rangle$	4.146 972 44(58)	0.929 472 295 02(6)
$\langle r_{12} \rangle$	7.083 427 6(12)	1.422 070 255 93(38)
$\langle 1/r_1 \rangle$	0.578 108 619(11)	1.688 316 800 5(6)
$\langle 1/r_{12} \rangle$	0.223 374 112(19)	0.945 818 448 5(6)
$\langle 1/r_1^2 \rangle$	0.873 035 760 4(46)	6.017 408 866 1(36)
$\langle 1/r_{12}^2 \rangle$	0.085 788 151 9(80)	1.464 770 922 4(15)
$\langle 1/r_1 r_2 \rangle$	0.239 016 167(21)	2.708 655 473 6(20)
$\langle 1/r_1 r_{12} \rangle$	0.154 038 646(14)	1.920 943 921 1(13)
$\langle \delta(r_1) \rangle$	0.157 506 390 55(31)	1.810 429 318 2(12)
$\langle \delta(r_{12}) \rangle$	0.001 473 985 59(13)	0.106 345 370 53(33)

TABLE II. Expectation values in atomic units. Uncertainties in the last digit(s) are given by the number in parentheses.

where $\tilde{y} = (2y)^4/\sqrt{1+(2y)^6}$, $a = 4\sqrt{2|\xi_c|}$, $n_0 = 2\langle\delta(r_1)\rangle$, and the fit parameters (c_k's and d_k's) are given in Tab. I. The short-range part is exact to first order in r and along with the long-range part contains higher order corrections to order r^9 by fitting to the pseudospectral density. The long-range part is chosen to reproduce Eq. (5) to order r^{-2} (second order), while the last term is a Padé approximant to the remaining error. Our numerical densities appear in appendix B. We believe that there is great value in parametrizations that capture asymptotic limits, which is why we constructed our critical density in such detail. Analytic forms can be applied in almost any context, and guarantees of asymptotic correctness can be useful in testing methods.

IV. EXPECTATION VALUES

We give expectation values of some simple operators in Table II, compared to those for the helium atom. At Z_C, the two-electron atom is much fatter than for $Z = 2$. Furthermore, the two electrons are much more likely to be on opposite sides of the nucleus than for $Z = 2$, as the expectation value of $\boldsymbol{r}_1 \cdot \boldsymbol{r}_2$ is more than an order of magnitude greater. We challenge any other method to match the precision of this table.

	Pseudospectral	fit
N	1.9999118	1.99757
E	-0.414 986 212 52(5)	
$E_{\rm H}$	0.595 467(52)	0.595 038
$T_{\rm S}$	0.389 857(17)	0.389 873
E_n	-1.053 346 537(20)	-1.053 176
$E_{\rm C}$	-0.049 240(39)	-0.049 202
$T_{\rm C}$	0.025 129(17)	0.0251 133

TABLE III. Normalization and energy components (total, Hartree, Kohn-Sham kinetic, nuclear, correlation, and kinetic correlation) of the critically bound system in atomic units. Uncertainties in the last digit(s) are given by the number in parentheses.

V. EXAMPLE BENCHMARKS FOR DENSITY FUNCTIONAL THEORY

To illustrate the usefulness of these results, we examine the behavior of the critical ion in KS DFT. For two unpolarized electrons, the ground-state energy and all exact KS energy components can be extracted directly from the density and external potential without solving an interacting problem by using the asymptotic decay of the density to determine the ionization potential and the virial theorem [16, 41]. We perform this procedure here as a test of the accuracy of our densities. These energies are listed in Table III for $Z = Z_c$ for both our pseudospectral density and our parametrized form [Eq. (8)]. The errors in the fit components are $\sim 0.1\%$ or less.

Next, we illustrate the usefulness of our method in explaining the behavior of approximations to DFT. At first glance, this system appears as a disaster for commonly used approximations, since their self-consistent densities will not bind the electrons. However, this is solely due to failures in the approximate $v_{\rm XC}(\mathbf{r})$, while the energy itself

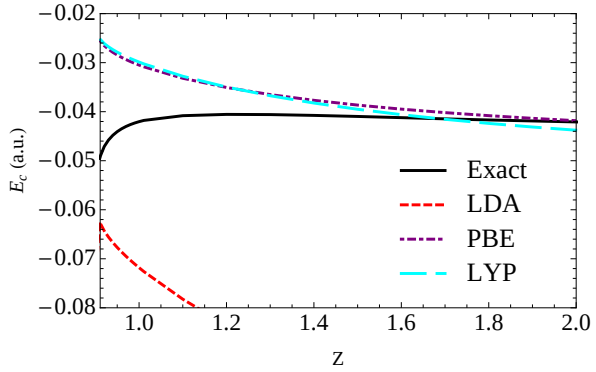

FIG. 2. (Color online) Exact and approximate correlation energies, evaluated with the exact densities.

remains highly accurate[42]. Evaluation on the accurate density circumvents this (important) distraction. In Fig. 2, we show several common $E_{\rm C}$ functionals for the two-electron ions, showing how unusual this system is. The LDA usually overestimates $E_{\rm C}$ by a factor of 2-3 (as it does for He), but here is *more accurate* than the "better" GGA approximations, PBE and LYP[43, 44]. This is clearly due to the sharp dip in the exact curve which occurs only for $Z \leq 1$. This oddness is also reflected in the ratio of $T_{\rm C}/|E_{\rm C}|$, which is close to 1 for He, close to 0 for stretched H_2, but close to 1/2 at $Z_{\rm C}$.

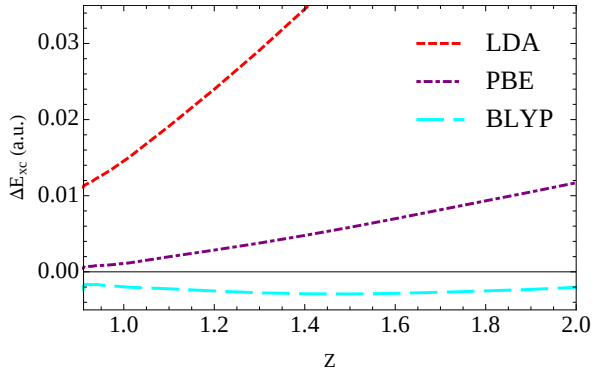

FIG. 3. (Color online) Error in approximations evaluated with the exact densities. For PBE at $Z = Z_c$, the error is 0.6 mhartree.

But DFT requires approximating both $E_{\rm X}$ and $E_{\rm C}$ simultaneously, and is notorious for cancellations of errors. In Fig. 3, we plot the XC errors, showing a very different picture. The GGA's are absurdly accurate, with errors that are far less than for $E_{\rm X}$ or $E_{\rm C}$ separately. How can we understand this? The clue is in the LDA result, which is remarkably accurate. For large Z (even He), $E_{\rm X}/E_{\rm C} >> 1$, so any cancellation is negligible. As Z reduces to $Z_{\rm C}$, $E_{\rm X}$ becomes much smaller, allowing a much greater cancellation. To see why this is so, in Fig. 4, we plot the system-averaged X, C, and XC holes of $Z = Z_{\rm C}$ and $Z = 1$[45]. The much smaller X hole at $Z_{\rm C}$ is much more greatly affected by the addition of the C hole, and the extent of the XC hole is much more short-ranged than that of X (or C) alone. Bringing the XC hole inwards makes it more amenable to local approximation, because of the accuracy of the ontop hole and cusp condition satisfied by LDA and PBE. This is why these approximations work unusually well for such a strongly correlated system.

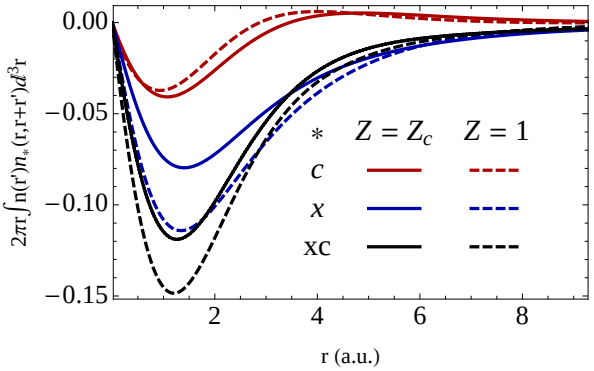

FIG. 4. (Color online) Exact density-weighted holes for $Z = Z_c$ and 1. The magnitude of the exchange hole decreases as $Z \to Z_c$, allowing for the error cancellation.

VI. CONCLUSIONS

We close with a clear illustration of the demands of this system, and the limits of even this method. Although the dependence of $v_{\rm S}(\mathbf{r})$ is notoriously sensitive to $n(\mathbf{r})$, a plot of $v_{\rm C}(\mathbf{r})$ for our fit density is indistinguishable from the numerical result. But in Fig. 5, we show $r^4\, v_{\rm C}(r)$, which is known to approach $-9/(4Z_{\rm C}^4)$ as $r \to \infty$. Our numerical density is accurate just far enough (to $r \approx 40$) to roughly meet the asymptote for $v_{\rm C}(r)$, and suggests the final value is not reached even at $r = 100$. For this quantity, our fit fails around $r \approx 8$, despite the care in its construction.

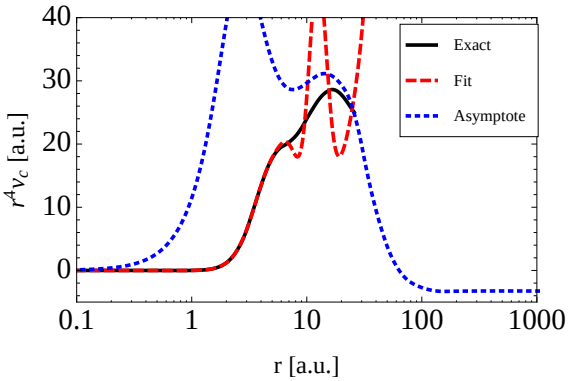

FIG. 5. (Color online) The correlation potential times r^4 calculated with our numerical density (exact, black), Eq. (8) (fit, dashed red), and using the asymptotic form 7 for the local noninteracting kinetic energy and the fit for the exchange energy (dotted, blue). Only by combining the asymptote with our exact data can we extract the behavior for all r.

In summary, we have shown that pseudospectral methods yield highly accurate densities, even at and near a quantum critical transition, allowing unprecedented evaluation of densities in the tail and of other position expectation values for such a situation. We have constructed high order asymptotic forms for all $Z \geq Z_c$ and used our densities to give accurate fits of the ionization energy and normalization factors in such expressions as a function of Z. A highly accurate fit for the critical density has been given to make this benchmark easier to use for other electronic structure theorists, and we demonstrate how this system can be used to evaluate and learn about errors with density functional theory examples. We have shown a remarkable cancellation of exchange and correlation errors for local and semi-local functionals at the critical density and explain this cancellation in terms of the exchange and correlation holes.

VII. ACKNOWLEDGEMENT

We gratefully acknowledge funding from the National Science Foundation (grant number CHE-1112442).

Appendix A: Errors in Asymptotic Densities

We have given the asymptotic densities at large r for all $Z \geq Z_c$ in Eqs. (4) and (7). These along with our fit to the normalization factors [Eq. (5) and $B = 0.1375$] and ionization energies [Eq. (6)] are useful for checking the accuracy of the electronic structure of any two-electron atom. Although these are exact expressions (up to the fits), there is still the open question of how accurate each order is as a function of r. We answer this question in detail in Fig. 6 for $Z = Z_c, 1$, and 2. There is no easily discernible pattern other than lower Z implies larger r for a given order. It is of note that the most well known asymptotic form (the zeroth-order expression) is relatively slow to converge to the exact density. For example, at $Z = Z_c$, it still yields a 10% error at $r = 50$ a.u.

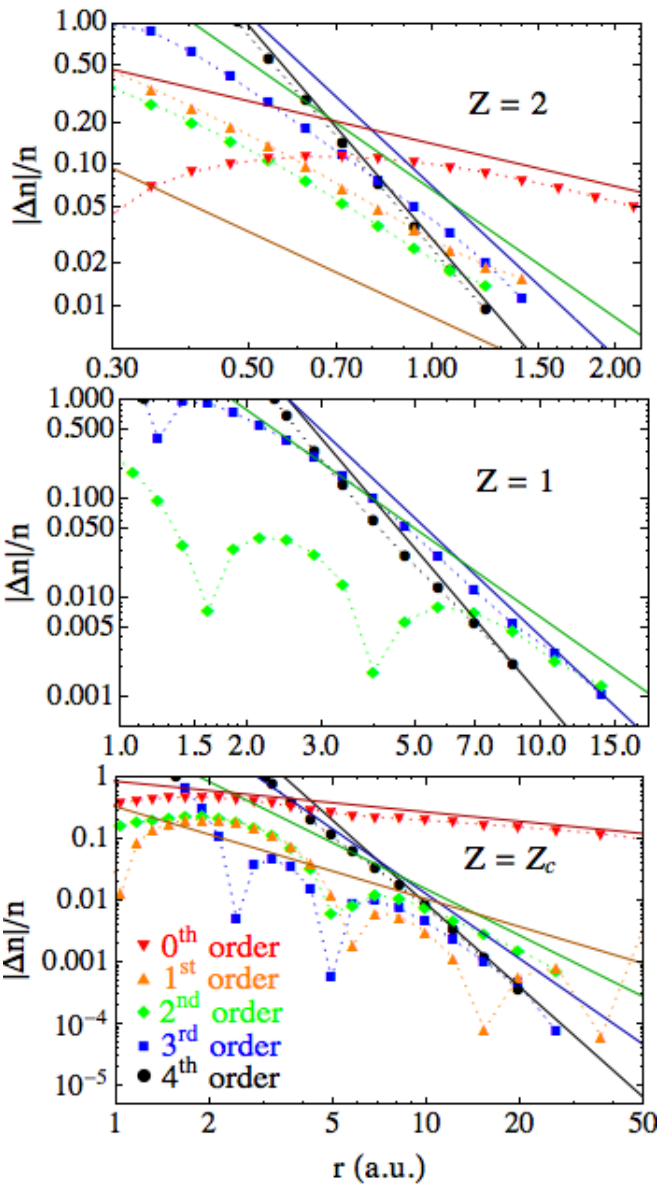

FIG. 6. (Color online) Relative error in the asymptotic densities [Eqs. (4) and (7)] compared to the exact densities (points) from zeroth to fourth order in $1/r$. The leading order correction to these formulas is calculated with higher order terms and plotted as dark solid lines except for the 4th order error which is made with a fit. These lines indicate whether the errors have reached the asymptotic regime or not. Note, that for $Z = 1$, zeroth, first, and second order are the same. There does not appear to be a general pattern. Deviations from limits at very large r are due to the limits in machine-precision arithmetic in calculating Ψ in the tail.

Appendix B: Raw Density Data

In the main body of the paper, we gave a fit to our density at $Z = Z_c$. This fit gave DFT energies to 0.1% or less. For those readers requiring more accuracy, we provide our best calculation of the one-electron density in Tab. IV. The accuracy of these data can be inferred from the value of our normalization in Tab. II, which is off by 9×10^{-5}. The majority of this error comes from the relatively large errors in the tail of the density. Since the weight for the density at the furthest out nonzero value is about 3×10^6, the error in the density values is about 3×10^{-11}, comparable to the error in our value of Z_c.

In order to obtain a functional form that can be easily evaluated off the grid or used to calculate derivatives, one should construct the Cardinal functions:

$$C_j(x) = \prod_{k=1,k\neq j}^{N} \frac{x - x_k}{x_j - x_k}, \tag{B1}$$

where $x = (1 - Z_c r)/(1 + Z_c r)$ and $N = 52$, which have the property of being equal to one at one grid point and zero at all the others. The density at an arbitrary value of x can then be obtained by

$$n(x) = \sum_{k=1}^{N} n_j C_j(x), \tag{B2}$$

the explicit values used for n_j are in Tab. IV (note, values in the table are divided by Z_c^3).

Integration can be performed via quadrature. The values of x_j are the Gaussian quadrature points (roots of the 53^{rd} order Legendre polynomial). For example,

$$\int d\boldsymbol{r} n(r) = \frac{1}{Z_c^3} \sum_{j=1}^{N} w_j n_j, \tag{B3}$$

where the values of w_j can be found in Tab. IV. Note, that the volume element $4\pi r^2 dr$ and the conversion from the r-coordinate to x-coordinate have already been taken into account by the values of w_j. Since the weights get rather large when r_j is big and the precision of the density is not very good in the tail, one should be careful about including such points in the quadrature. Usually some sort of truncation scheme is needed, chosen at a value of r such that contributions from larger r should be negligible.

r_j (a.u.)	x_j (a.u.)	n_j/Z_c^3 (a.u.)	w_j (a.u.)
0.0005759641912909017	0.9989511111039503	0.314682351915279	$4.660741235847267\times10^{-9}$
0.00303925808565137	0.9944775909292161	0.3132732840892592	$3.0300099503007153\times10^{-7}$
0.007489495670215863	0.9864461956515499	0.3107441016739011	$2.9066843483625716\times10^{-6}$
0.013959796221790716	0.9748838842217445	0.30710436909115857	0.00001387789094030296
0.02249735397316229	0.9598318269330866	0.3023689171597749	0.0000461234044816 1165
0.03316494107684804	0.9413438536413591	0.29655769404226007	0.0001228806422910 7963
0.046041970051123156	0.9194861289164246	0.28969610387322686	0.0002822492302942 0383
0.061225781649952314	0.8943368905344953	0.2818154628129142	0.000583230852029 3945
0.07883324279239258	0.8659861628460676	0.27295353887455004	0.0011139006628788277
0.09900270777331016	0.8345354323267345	0.2631551627930131	0.0020025658396714803
0.12189640224230178	0.8000972834304684	0.252472896572073	0.0034331010464428006
0.147703303023036	0.7627949951937449	0.24096774168832766	0.005666131691016764
0.17664260478943944	0.7227620997499832	0.22870986212496724	0.009068430900444735
0.2089678872961224	0.6801419042271677	0.21577928855460538	0.014153905827555817
0.24497212550105105	0.6350869776952459	0.20226655892230294	0.021641025428937748
0.28499372130027406	0.5877586049795791	0.18827323726105366	0.032533717316659924
0.32942378214164697	0.5383262092858274	0.17391223683317283	0.04823599283798371
0.3787149317776135	0.48696674569809606	0.15930785598077488	0.07071540224691103
0.43339201631982543	0.4338640677187617	0.14459541626218037	0.10273774745849322
0.4940651706915445	0.3792082691160937	0.12992037421715608	0.1482066729138109
0.5614458450037321	0.32319500343480784	0.11543676326001442	0.21265904048506942
0.6363665691262939	0.2660247836050018	0.10130481511247609	0.30399399290119455
0.7198054734468116	0.20790226415636606	0.0876876171812794	0.43355629325257544
0.8129169082310087	0.14903550860694917	0.07474669189818135	0.6177628843571673
0.9170699472802668	0.08963524464890056	0.06263644690028392	0.8805726039488526
1.033897173471482	0.029914109797338766	0.05149755279322456	1.2572818945152056
1.1653569976191294	-0.029914109797338766	0.04144946858019295	1.800435561708559
1.3138139675134421	-0.08963524464890056	0.032582558170176246	2.5891630981063303
1.4821432470208165	-0.14903550860694917	0.02495051560492449	3.744155528864454
1.6738679412287918	-0.20790226415636606	0.018564108415709536	5.452097769788892
1.8933416121746534	-0.2660247836050018	0.013387488441818883	8.006263376861513
2.145993806251467	-0.32319500343480784	0.009338394879270824	11.875328334071545
2.4386647296695396	-0.3792082691160937	0.006293338088208658	17.822611142279463
2.7800680689846717	-0.4338640677187617	0.004097904475823055	27.117747215953976
3.1814412499350295	-0.48696674569809606	0.002583092692168 3018	41.92262357320114
3.657475177082267	-0.5383262092858274	0.001580782753423 7687	66.01620223603643
4.2276696497961455	-0.5877586049795791	0.000941559913449 2133	106.20157190068788
4.9183526634276635	-0.6350869776952459	0.000545304228261 0736	175.1405955662702
5.76576296728434	-0.6801419042271677	0.000304999786938 1752	297.30896094699824
6.820887335531765	-0.7227620997499832	0.000162420827538 32506	522.1176753124039
8.157294259937565	-0.7627949951937449	0.000080775889813 59748	954.4527398959269
9.884289312564363	-0.8000972834304684	0.000036650634880 89955	1830.417963708067
12.169963155779914	-0.8345354323267345	0.000014740319797 992315	3719.7467675090556
15.28364511271759	-0.8659861628460676	$5.054109250994349\times10^{-6}$	8117.066837845993
19.678953431941505	-0.8943368905344953	$1.3947108874720773\times10^{-6}$	19366.157899552323
26.168717467688783	-0.9194861289164246	$2.8316551169626493\times10^{-7}$	51822.50322060266
36.329306394116436	-0.9413438536413591	$3.6357597278623005\times10^{-8}$	161516.57680062292
53.55560068801603	-0.9598318269330866	$2.2296122675325307\times10^{-9}$	622216.7754332445
86.30923308485625	-0.9748838842217445	$3.32223667644662\times10^{-11}$	$3.2798803957197545\times10^{6}$
160.8732228413056	-0.9864461956515499	0.	$2.880656250507084\times10^{7}$
396.4320475486722	-0.9944775909292161	0.	$6.724307713324147\times10^{8}$
2091.8996773448594	-0.9989511111039503	0.	$2.2330122223506357\times10^{11}$

TABLE IV. Density at the pseudospectral grid points and quadrature weights.

[1] V. E. A. Hylleraas, Z. Phys. **54**, 347 (1929).
[2] C. L. Pekeris, Phys. Rev. **112**, 1649 (1958).
[3] C. Schwartz, Int. J. of Mod. Phys. E **15**, 877 (2006).
[4] H. Nakashima and H. Nakatsuji, J. Chem. Phys. **127**, 224104 (2007).
[5] H. Nakashima and H. Nakatsuji, J. Chem. Phys. **128**, 154107 (2008).
[6] Y. I. Kurokawa, H. Nakashima, and H. Nakatsuji, Phys. Chem. Chem. Phys. **10**, 4486 (2008).
[7] P. Serra and S. Kais, Phys. Rev. Lett. **77**, 466 (1996).
[8] J. P. Neirotti, P. Serra, and S. Kais, Phys. Rev. Lett. **79**, 3142 (1997).
[9] C. S. Estienne, M. Busuttil, A. Moini, and G. W. F. Drake, Phys. Rev. Lett. **112**, 173001 (2014).
[10] A. Mirtschink, C. J. Umrigar, J. D. Morgan, and P. Gori-Giorgi, The Journal of Chemical Physics **140**, 18A532 (2014).
[11] J. D. Baker, D. E. Freund, R. N. Hill, and J. D. Morgan, Phys. Rev. A **41**, 1247 (1990).
[12] I. A. Ivanov, Phys. Rev. A **51**, 1080 (1995).
[13] A. V. Sergeev and S. Kais, Journal of Physics A: Mathematical and General **32**, 6891 (1999).
[14] C. Schwartz, "Perturbation theory and threshold bound state for two electron atom," unpublished (2013).
[15] G. W. F. Drake, in *Atomic, Molecular, and Optical Physics Handbook*, edited by G. W. F. Drake (American Institute of Physics, 1996).
[16] C. J. Umrigar and X. Gonze, Phys. Rev. A **50**, 3827 (1994).
[17] C.-J. Huang and C. J. Umrigar, Phys. Rev. A **56**, 290 (1997).
[18] S. J. A. van Gisbergen, F. Kootstra, P. R. T. Schipper, O. V. Gritsenko, J. G. Snijders, and E. J. Baerends, Phys. Rev. A **57**, 2556 (1998).
[19] H. Appel, E. K. U. Gross, and K. Burke, Phys. Rev. Lett. **90**, 043005 (2003).
[20] W. H. Press, S. A. Teukolsky, W. T. Vetterling, and B. P. Flannery, *Numerical Recipes: The Art of Scientific Computing*, third edition ed. (Cambridge University Press, 32 Avenue of the Americas, New York, NY 10013-2473, USA, 2007).
[21] C. Canuto, M. Hussaini, A. Quarteroni, and T. Zang, *Spectral Methods in Fluid Dynamics* (Springer, Berlin, 1988).
[22] L. E. Kidder and L. S. Finn, Phys Rev. D **62**, 084026 (2000).
[23] H. P. Pfeiffer, L. E. Kidder, M. A. Scheel, and S. A. Teukolsky, Comput. Phys. Commun. **152**, 253 (2003).
[24] R. A. Friesner, Chem. Phys. Lett. **116**, 39 (1985).
[25] R. A. Friesner, J. Chem. Phys. **85**, 1462 (1986).
[26] R. A. Friesner, J. Chem. Phys. **86**, 3522 (1987).
[27] M. N. Ringnalda, M. Belhadj, and R. A. Friesner, J. Chem. Phys. **93**, 3397 (1990).
[28] B. H. Greeley, T. V. Russo, D. T. Mainz, R. A. Friesner, J.-M. Langlois, W. A. Goddard, III, J. Robert E. Donnelly, and M. N. Ringnalda, J. Chem. Phys. **101**, 4028 (1994).
[29] R. B. Murphy, M. D. Beachy, R. A. Friesner, and M. N. Ringnalda, J. Chem. Phys. **103**, 1481 (1995).
[30] R. B. Murphy, Y. Cao, M. D. Beachy, M. N. Ringnalda, and R. A. Friesner, J. Chem. Phys. **112**, 10131 (2000).
[31] C. Ko, D. K. Malick, D. A. Braden, R. A. Friesner, and T. J. Martínez, J. Chem. Phys. **128**, 104103 (2008).
[32] J. S. Heyl and A. Thirumalai, Mon. Not. R. Astron. Soc. (2010).
[33] A. G. Borisov, J. Chem. Phys. **114**, 7770 (2001).
[34] J. P. Boyd, C. Rangan, and P. H. Bucksbaum, J. Comput. Phys. **188**, 56 (2003).
[35] P. E. Grabowski and D. F. Chernoff, Phys. Rev. A **81**, 032508 (2010).
[36] P. E. Grabowski and D. F. Chernoff, Phys. Rev. A **84**, 042505 (2011).
[37] J. P. Perdew, R. G. Parr, M. Levy, and J. L. Balduz, Phys. Rev. Lett. **49**, 1691 (1982).
[38] R. M. Dreizler and E. K. U. Gross, *Density Functional Theory: An Approach to the Quantum Many-Body Problem* (Springer–Verlag, Berlin, 1990).
[39] C. Amovilli and N. H. March, Journal of Physics A: Mathematical and General **39**, 7349 (2006).
[40] M. Hoffmann-Ostenhof, T. Hoffmann-Ostenhof, and B. Simon, Journal of Physics A: Mathematical and General **16**, 1125 (1983).
[41] N. T. Maitra, K. Burke, H. Appel, E. K. U. Gross, and R. van Leeuwen, "Ten topical questions in time-dependent density functional theory," in *Reviews in Modern Quantum Chemistry: A Celebration of the Contributions of R.G. Parr*, edited by K. Sen (World Scientific, 2001) pp. 1186–1225.
[42] M.-C. Kim, E. Sim, and K. Burke, Phys. Rev. Lett. **111**, 073003 (2013).
[43] C. Lee, W. Yang, and R. G. Parr, Phys. Rev. B **37**, 785 (1988).
[44] B. Miehlich, A. Savin, H. Stoll, and H. Preuss, Chem. Phys. Lett. **157**, 200 (1989).
[45] K. Burke, J. P. Perdew, and M. Ernzerhof, The Journal of Chemical Physics **109**, 3760 (1998).